The Astrophysical Journal, 703:500–506, 2009 September 20 doi:10.1088/0004-637X/703/1/500

ANALYSIS OF BREIT–PAULI TRANSITION PROBABILITIES FOR LINES IN O III

C. Froese Fischer[1], G. Tachiev[2], R. H. Rubin[3,4,5], and M. Rodríguez[6]
[1] National Institute of Standards and Technology, Gaithersburg, MD 20899-8422, USA; charlotte.fischer@nist.gov
[2] Florida International University, Miami, FL, USA
[3] NASA Ames Research Center, Moffett Field, CA 94035-1000, USA
[4] Orion Enterprises, M.S. 245-6, Moffett Field, CA 94035-1000, USA
[5] Kavli Institute for Astronomy and Astrophysics, Peking University, Beijing 100871, China
[6] Instituto Nacional de Astrofísica, Óptica y Electrónica, Apdo Postal 51 y 216, 72000 Puebla, Mexico
Received 2009 May 27; accepted 2009 June 22; published 2009 August 28

ABSTRACT

Accurate atomic data are essential for understanding the properties of both O III lines produced by the Bowen fluorescence mechanism and [O III] forbidden lines observed in numerous gaseous nebulae. Improved Breit–Pauli transition probabilities have been published for the carbon sequence. Included were revised data for O III. The present paper analyzes the accuracy of the data specifically for O III by comparison with other theory as well as some recent experiments and observations. For the electric dipole transition probabilities, good agreement is found for allowed Bowen fluorescence lines between predictions of intensity ratios with observed data. For forbidden transitions, the Breit–Pauli magnetic dipole transition operator requires corrections that often are neglected. Good agreement is found when these transition probabilities are computed with multiconfiguration Dirac–Hartree–Fock methods.

Key words: atomic data – atomic processes

Online-only material: color figures

1. INTRODUCTION

Uncertainties in the atomic data are one of the main sources of errors in astrophysical calculations. The uncertainties arise even when the atomic data are derived from detailed quantum mechanical computations, since they rely on several approximations whose reliability is difficult to assess. Among the more relevant atomic data are those for O III, because this ion plays a central role in the determination of the O abundance in photoionized gas, and O abundances are widely used as a proxy for the metallicity of the interstellar medium. In this context, objects like Orion Nebula or the RR Telescopii, where a large number of O III lines can be measured, are very useful, in particular when several of the measured lines arise from the same upper level and can be used to assess the reliability of the calculated transition probabilities. Reliable values of transition probabilities can be used, in turn, to check on the procedure used to assign errors to the measurements of line intensities, which is not always an easy task.

RR Telescopii is a slowly evolving nova (and often called a symbiotic star), still in the nebular stage, with a number of intriguing features including a rich and complex emission spectrum over a wide range of ionization and excitation energies. Recently Selvelli et al. (2007) reported the results of their analysis of the He II Fowler lines and the O III and N III Bowen fluorescence lines in this nova. For their analysis they combined the most recent observed data from the Space Telescope Imaging Spectrograph (STIS) at the *Hubble Space Telescope* (*HST*) and the Ultraviolet and Visual Echelle Spectrograph (UVES) at the Very Large Telescope in order to exploit the best characteristics of these instruments. This allowed them to obtain reliable emission-line intensities and line ratios that included some weak O III lines. For their analysis they relied on radiative rates taken primarily from a review by Kastner & Bhatia (1996).

Bowen fluorescence and its role in nebulae, the sun, Scorpius X-1, and laboratory plasma was studied by Kastner & Bhatia (1990) who also derived a number of explicit formulae for analysis. Transition rates and collision strengths for O III were reported (Bhatia & Kastner 1993) from a calculation using a distorted wave approximation. These data were necessary for an investigation of level population and line intensities. The following year, transition data became available (Froese Fischer 1994) from variational multiconfiguration Hartree–Fock (MCHF) calculations that included both one- and two-body relativistic operators in the Breit–Pauli approximation. The Kastner & Bhatia (1996) paper is an overview and a re-analysis of the observations relating to the Bowen fluorescence. Considerable differences were found in the transition rates from the two theoretical calculations. A comparison (Selvelli et al. 2007) of the observed (STIS and UVES) and predicted intensity ratios for pairs of Bowen lines originating from the same upper level showed that the ratios from observed data agreed best (though not perfectly) with those derived from the Breit–Pauli data. At the same time, Selvelli et al. (2007) pointed out that the values in the Atomic Spectroscopy Database (ASD) at the National Institute of Standards (NIST) differ by about 10% from the Breit–Pauli values.

The present online ASD (Ralchenko et al. 2008) values were published some time ago as critically evaluated data (Wiese et al. 1994). The values were derived from LS calculations by Luo et al. (1989) at the University College, London and no longer represent the most accurate values. The Breit–Pauli values mentioned earlier were improved as part of a project for the systematic calculation of energy levels, lifetimes, and transition probabilities for the carbon sequence as well as others. The computational procedure and a general analysis of the accuracy of the results for the sequence were presented (Tachiev & Froese Fischer 2001). The E1 transition rates (A_{ki}) important to Bowen fluorescence were compared with other theory, but the emphasis was on the evaluation of data for the sequence rather than O III in particular. Data for all transitions in O III from levels between the ground state and the $2p^4\ ^1S_0$ excited level, except for $2s2p^23s\ ^5P$ term, were also included in a subsequent publication for the beryllium to neon isoelectronic sequences

(Froese Fischer & Tachiev 2004). All results are available at a Web site (Froese Fischer & Tachiev 2002).

In this paper, we revisit the O III calculations for a more complete evaluation. For brevity we shall refer to the O III energy adjusted data in these three sources as TFF without further reference. We begin with a brief review of the computational procedure that was used, present the ab initio energy levels and their accuracy, and then compare the transition probability from the *energy adjusted* data with both theoretical and experimental data, particularly new data that may have been reported in the interim. To the extent that the question of accuracy is related to the computational procedure, some comparisons are with experimental data for transitions not directly relevant to Bowen fluorescence.

2. COMPUTATIONAL PROCEDURE

In the Breit–Pauli approximation (Froese Fischer 1997), the wave function, Ψ, is a linear combination of configuration state functions (CSF) of the form

$$\Psi(\gamma J) = \sum_{LS} \sum_{j} c_j(LSJ)\Phi(\gamma_j LSJ), \qquad (1)$$

where γ usually represents the dominant configuration and any additional quantum numbers required in order to uniquely specifying the state. The CSFs, $\Phi(\gamma_j LSJ)$, for a configuration and its coupling γ_j, term LS, and total angular momenta L and S coupled to J, are built from a basis of one-electron spin orbitals,

$$\phi_{nlm_l m_s} = \frac{1}{r} P_{nl}(r) Y_{lm_l}(\theta, \varphi)\chi_{m_s}, \qquad (2)$$

where $P_{nl}(r)$ is a radial wave function. The expansion coefficients, $c_j(LSJ)$, and the corresponding energy, $E(LSJ)$, are an eigenvector and eigenvalue, respectively, of the interaction matrix of these CSFs as defined by the Breit–Pauli Hamiltonian. The computer code used was the atomic structure package, ATSP2K (Froese Fischer et al. 2007). All two-body operators were included in these calculations except for the orbit–orbit operator whose effect is negligible.

The accuracy of the final result depends on the accuracy of the radial functions as well as the set of CSFs. The ATSP2K code is based on the MCHF approach for obtaining the "best" radial functions for the orbital set. The wave function expansion included all single and double excitations from the dominant configuration of the wave function with the restriction that all CSFs contain at least one $1s$ electron. Selected triple and quadruple excitations were also included to account for near degeneracy. Wave functions were obtained for all levels up to the $2p^4\ {}^1S_0$ level, except for the $2s2p^2 3s\ {}^5P$ term. Further details may be found in Tachiev & Froese Fischer (2001).

The results of an ab initio calculation are useful in that the error with respect to observed energy levels as well as agreement between the length and velocity values of the line strength can be used as an indicator of accuracy. But ab initio values can be improved by adjusting the energy of a selected level of a term to agree with its observed value. Such "fine-tuning" has been shown to improve the computed oscillator strengths (Fleming et al. 1994) since it improves the LSJ composition of the wave function. In addition, the calculation of transition rates is then based on theoretical wavelengths (in vacuum). However, the accuracy of energy levels from such a process cannot be used as an indication of accuracy since they are semiempirical, although the fine-structure splitting is still ab initio.

Table 1
Observed Energy Levels (in cm^{-1}), Difference of Computed (ab initio) from Observed (Ralchenko et al. 2008) (Computed—Observed), and Lifetimes τ

Config.	Term	J	Obs.	Diff.	τ (in s)
$2s^22p^2$	^3P	0	0.00		
		1	113.18	0.19	3.85(+04)
		2	306.17	−0.57	1.04(+04)
$2s^22p^2$	^1D	2	20273	96	3.67(+01)
$2s^22p^2$	^1S	0	43186	92	5.23(−01)
$2s2p^3$	$^5S^o$	2	60325	207	1.24(−03)
$2s2p^3$	$^3D^o$	3	120025	439	1.63(−09)
		2	120053	439	1.62(−09)
		1	120058	440	1.62(−09)
$2s2p^3$	$^3P^o$	2	142381	522	5.44(−10)
		1	142382	524	5.43(−10)
		0	142394	526	5.42(−10)
$2s2p^3$	$^1D^o$	2	187054	612	1.83(−10)
$2s2p^3$	$^3S^o$	1	197088	494	6.99(−11)
$2s2p^3$	$^1P^o$	1	210462	723	9.18(−11)
$2s^22p3s$	$^3P^o$	0	267259	583	2.55(−10)
		1	267377	583	2.55(−10)
		2	267634	582	2.55(−10)
$2s^22p3s$	$^1P^o$	1	273081	639	2.14(−10)
$2p^4$	^3P	2	283760	936	1.65(−10)
		1	283977	934	1.65(−10)
		0	284072	934	1.65(−10)
$2s^22p3p$	^1P	1	290958	714	8.73(−09)
$2s^22p3p$	^3D	1	293866	711	5.38(−09)
		2	294003	710	5.36(−09)
		3	294223	709	5.35(−09)
$2s^22p3p$	^3S	1	297559	670	2.37(−09)
$2p^4$	^1D	2	298294	1098	4.26(−10)
$2s^22p3p$	^3P	0	300230	677	2.95(−09)
		1	300312	677	2.94(−09)
		2	300443	676	2.92(−09)
$2s^22p3p$	^1D	2	306586	736	3.45(−09)
$2s^22p3p$	^1S	0	313803	869	1.70(−09)
$2s^22p3d$	$^3F^o$	2	324465	647	3.41(−10)
		3	324661	652	4.10(−09)
		4	324839	651	5.13(−09)
$2s^22p3d$	$^1D^o$	2	324736	638	1.40(−10)
$2s^22p3d$	$^3D^o$	1	327229	598	4.87(−11)
		2	327278	598	4.88(−11)
		3	327352	598	4.88(−11)
$2s^22p3d$	$^3P^o$	2	329470	608	8.36(−11)
		1	329584	608	8.36(−11)
		0	329645	608	8.37(−11)
$2s^22p3d$	$^1F^o$	3	331821	631	5.04(−11)
$2s^22p3d$	$^1P^o$	1	332779	641	8.11(−11)
$2p^4$	^1S	0	343306	1455	1.68(−10)

3. ENERGY LEVELS AND LIFETIMES

Table 1 lists the observed energy levels, the difference of the computed ab initio energy levels and observed levels, and the lifetime of the levels from the adjusted wave functions. The lifetimes are computed from E1 transitions for excited configurations and E2 and M1 transitions for levels of the $2s^22p^2$ ground configuration. The largest discrepancies between computed and observed energy levels are for the $2p^4\ {}^1S_0$ and $^1D_2$ states for which larger expansions are needed to reach the same level of accuracy in the energy as the ground state. The previous (Froese Fischer 1994) calculation included only the $2p^4\ {}^3P$ term and was in error by about 2440 cm^{-1}. In the present calculation this error has been reduced to 936 cm^{-1} and the calculation was extended to include also the other terms. There

Table 2
Lifetimes from Theory and Experiment

Level		TFF	Other Theory		Exp.
$2s^2 2p^2$	$^1S_0$	525[a]			530 ± 15[b]
					540 ± 27[c]
$2s2p^3$	$^5S^o_2$	1.24	1.21[d]		1.22 ± 0.08[e]
$2s2p^3$	$^3D^o$	1.62	1.57[f]	1.63[g]	1.61 ± 0.06[h]
	$^3P^o$	0.544	0.434[f]	0.530[g]	0.575 ± 0.018[h]
	$^1D^o$	0.183	0.175[f]	0.183[g]	0.20 ± 0.05[h]
	$^3S^o$	0.070	0.064[f]	0.069[g]	0.079 ± 0.04[h]
	$^1P^o$	0.092	0.080[f]	0.090[g]	0.087 ± 0.011[h]
$2p3s$	$^3P^o$	0.255	0.262[f]	0.253[g]	0.266 ± 0.011[i]
	$^1P^o$	0.214	0.228[f]	0.215[g]	0.227 ± 0.011[i]
				0.219[j]	0.17 ± 0.01[k]

Notes. Lifetimes for the first two levels are in 10^{-3} s whereas the rest are in 10^{-9} s.
[a]M1 rates from MCDHF calculations (see Section 7).
[b]Träbert et al. (2000).
[c]Smith et al. (2004).
[d]Fleming & Brage (1997).
[e]Johnson & Smith (1984).
[f]Nahar (1998).
[g]Luo et al. (1989).
[h]Pinnington et al. (1974).
[i]Pinnington et al. (1978).
[j]Aggarawal et al. (1997).
[k]Baudinet-Robinet et al. (1991).

is excellent agreement with the observed fine-structure splitting for the $2s^2 2p^2\ ^3P$ term when the two-body Breit–Pauli operators are included. These operators considerably increase the time required for the evaluation of matrix elements of the interaction matrix. Consequently, only the one-body operators are often included (see, for example, Nahar 1998). With such an assumption the $^3P_2$ energy level becomes 493 cm^{-1} instead of 306 cm^{-1}, thus vastly overestimating the relativistic correction.

Most experimental transition data is available only for the lifetimes of levels. The calculation of an accurate lifetime depends primarily on the accuracy of the strongest lines which generally are LS allowed transitions where cancellation in the line strength is not present and relativistic effects do not significantly affect the LS composition of the wave function. In O III the relativistic effects are sufficiently small that, to the accuracy reported, the lifetimes are not J-dependent. The only exceptions are the levels of $2p^2\ ^3P$ that decay through E2 and/or M1 transitions. Table 2 compares some present lifetimes of lower levels with close-coupling results and experiment.

The lifetime for the $2s^2 2p^2\ ^1S_0$ level has been measured accurately using a heavy-ion storage ring (Träbert et al. 2000) as an electron source and also an electron cyclotron ion source (Smith et al. 2004). Our computed lifetime, reported as 523 ms in Table 1 but corrected here by the use of the more accurate M1 transition rate (see Section 7) is in excellent agreement with both these measurements. The experimental lifetime of the metastable $^5S^o_2$ level, determined from the direct measurement of the time dependence of spontaneous emission of O^{+2} ions (Johnson & Smith 1984), is also in good agreement with our computed lifetime, all in ms.

The remaining lifetimes (in ns) in Table 2 are determined from E1 transition rates to lower levels. The most recent other theory values are those reported by Nahar (1998) that include only the one-body Breit–Pauli operators in a close-coupling approximation but the present results are actually in better agreement with the earlier LS calculation (Luo et al. 1989). Aggarawal et al. (1997) did not actually report lifetimes but in the case of $2p3s\ ^1P$ it can readily be determined and has been included in this table. This result too is in good agreement with our present value. The experimental values are from relatively early beam-foil measurements (Pinnington et al. 1974, 1978) with the exception of a more recent beam-foil-laser measurement (Baudinet-Robinet et al. 1991). All theory is essentially in agreement with experiment because of the relatively large error bars for the latter.

Table 3
Nonrelativistic $2p3p\ ^3D - 2p3d\ ^3P^o$ Transition Energies (ΔE in cm^{-1}) and Line Strengths ($S(L)$, $S(V)$) for Calculations of Increasing Size Where n Refers to the Largest Principal Quantum Number in the nl Orbital Set

n	ΔE	$S(L)$	$S(V)$	Disc.(%)
4	35049.52	1.87390	0.51133	72.7
5	35135.66	1.69727	0.81205	52.1
6	35179.49	1.66221	1.02719	38.2
7	35208.27	1.78911	1.39222	22.2

4. E1 TRANSITION RATES AND THEIR ACCURACY

Accurate transition probabilities for both allowed and intercombination transitions require a higher level of accuracy for the wave functions than do lifetimes. Indicators of accuracy (Froese Fischer 2009) are the errors in the transition energy and the discrepancy in the length, and velocity form of the line strength. They are not direct error estimates: theoretical transition energies may agree exactly with experiment without the wave functions being exact and similarly the length and velocity values of the line strength may be in exact agreement for an approximate wave function but agreement in both is an indication of accuracy. This general remark needs to be qualified. In nonrelativistic theory, the length and velocity forms of the line strength agree exactly for an exact solution of the wave equation, but the agreement no longer holds in the Breit–Pauli approximation (Froese Fischer 2009) when the nonrelativistic form of the transition operator is used to compute the line strength as is customary. However, most transitions in light atoms are sufficiently nonrelativistic that length and velocity are still useful indicators. In the present calculations, the transition rates from energy-adjusted calculations usually changed by only a few units in the third significant digit. This leaves the discrepancy in length and velocity values as the remaining indicator of accuracy.

The accuracy indicators can be viewed at the Web site http://atoms.vuse.vanderbilt.edu. A search for O III data (6 electrons and atomic number 8) for transitions between selected LS terms displays the wavelength in vacuum (in Å), the line strength S, the oscillator strength f in absorption, the transition probability in emission A_{ki} (in s^{-1}), and the discrepancy indicator in percent ($100(S_L - S_V)/\max(S_L, S_V)$). For many transitions, this is a fraction of 1.0%. For a few it is larger than 50%, usually because the transition rate is unexpectedly small. An example is the transition probability for the intercombination $2p3p\ ^1P_1 - 2p3d\ ^3P^o_0$ line. For many $2p3p - 2p3d$ triplet–triplet transitions, the discrepancy is a few percent, but for the $^3D - {}^3P^o$ multiplet the discrepancy ranges from 20%–33%. In such cases, it is helpful to review the LS convergence trend of a calculation. Table 3 shows the convergence of the transition energy and the line strengths ($S(L)$ and $S(V)$) as more and more orbitals are used in the description of the wave functions where n refers to

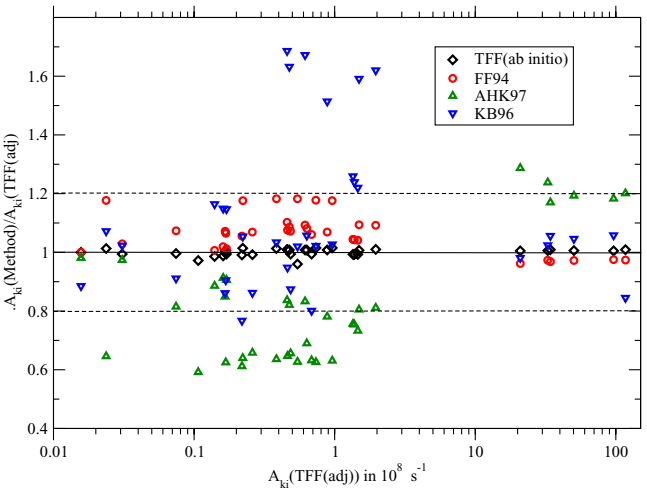

Figure 1. Comparison of some theoretical transition rates. Shown is the ratio of TFF (ab initio; Froese Fischer & Tachiev 2002), FF94 (Froese Fischer 1994), AHK97 (Aggarawal et al. 1997), KB96 (Kastner & Bhatia 1996) transition rates relative to TFF(adjusted) values as a function of the transition rate in 10^8 s^{-1}.
(A color version of this figure is available in the online journal.)

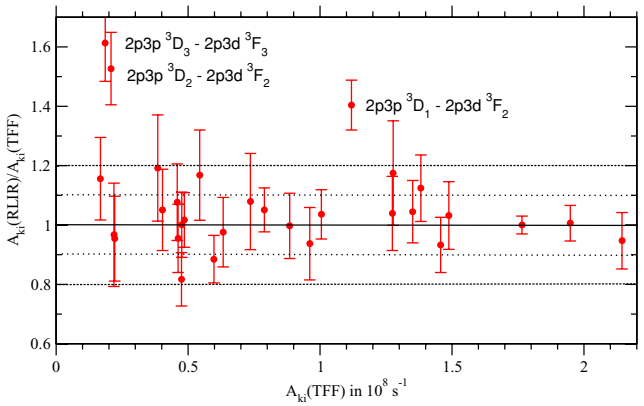

Figure 2. Comparison of theoretical and experimental transition rates derived from dimensionless RLIR values from experiment (Djeniže et al. 2003) as a function of theoretical values (Tachiev & Froese Fischer 2001).
(A color version of this figure is available in the online journal.)

the maximum n. This table shows that a computational problem is primarily associated with the velocity value which is steadily increasing. The line strength for the $^3D_2 - {}^3D_2^o$ is about 36 times larger than for $^3D_2 - {}^3P_2^o$. Thus, there might well be considerable cancellation in the calculation of the line strength of this transition (see Froese Fischer 1981 for a discussion of cancellation in the presence of configuration interaction).

Theoretical transition rates for the important lines for Bowen fluorescence listed by Kastner & Bhatia (1996; Table 3) are compared in Figure 1 with several misprints corrected. Shown are the ab initio results of Tachiev & Froese Fischer (2001) which differ only slightly from their energy adjusted values. For the larger transition rates, there is excellent agreement between the earlier Breit–Pauli (Froese Fischer 1994) and the distorted wave results of Bhatia & Kastner (1993). The smallest value in this figure is for the $2p3p\ ^3D_2 - 2p3d\ ^3P_2^o$ for which there is good agreement. For lines of intermediate value, many are within the 20% deviation shown by the dashed line, but others differ significantly.

5. EXPERIMENTAL E1 TRANSITION PROBABILITIES

Relative (dimensionless) transition probabilities for 15 O III multiplets have been reported by Djeniže et al. (2003) from laboratory experimental measurements. In most cases, these results are the first data obtained experimentally using the relative line intensity ratio (RLIR) method. Particularly recommended for astrophysical applications is the ratio of the 3313 Å ($2p3s\ ^3P_1^o - 2p3p\ ^3S_1$) line to the 3342 Å ($2p3s\ ^3P_2^o - 2p3p\ ^3S_1$) line. The intensity ratio of 0.723 is in excellent agreement with the value of 0.736 from the TFF Breit–Pauli data.

In their paper, relative transition probabilities are reported based on the assumption that the transition rate is unity for the $2p3p\ ^3D_2 - 2p3d\ ^3F_3^o$ transition. Figure 2 compares these relative transition rates multiplied by the TFF transition rate of 1.765×10^8 s^{-1} with values from present data as a function of the theoretical transition rate. Included are the singlet–singlet and triplet-triplet transitions with experimental error bars ranging from 3%–15%. The figure shows that the vast majority agree with the Breit–Pauli values to this accuracy. Exceptions are some of the $2p3p\ ^3D - 2p3d\ ^3F^o$ transitions not associated with Bowen fluorescence. It is not clear how error bars were determined. Frequently in experimental measurements, small transition rates have a larger relative error than those with large transition rates but Djeniže et al. (2003) assigned errors mainly by multiplet. In their paper, they compared their relative values with those from a number of other theories.

The determination of the $^3F_2^o$ wave function depends critically on how both correlation and relativistic effects are treated. In a Breit–Pauli calculation the first few terms of the wave function expansion (in decreasing order) are:

$$0.837\ 2s^2 2p3d\ ^3F_2^o + 0.492\ 2p^3 3d\ ^3F_2^o +$$
$$0.492\ 2s^2 2p3d\ ^1D_2^o + 0.093\ 2p^3 3d\ ^1D_2^o + \cdots$$

The $^1D_2^o$ component is large because the $^3F_2^o$ and $^1D_2^o$ levels are separated by only 271 cm^{-1} which is a small separation when compared with the $^3F_4^o - {}^3F_2^o$ fine-structure splitting of 374 cm^{-1}. In fact, the $^1D_2^o$ level is lower than the $^3F_4^o$ level. The present computed ab initio level separation already had a good value of 262 cm^{-1} and was improved in the adjusted data. The other theories may not have treated the relativistic effects as carefully which may explain the variation in theory. However, this does not explain the difference with experiment shown in Figure 2 and further studies are needed to resolve this discrepancy.

6. E1 LINE INTENSITY RATIOS

Relative intensities of observed lines with the same upper level can be compared directly to relative transition rates in that

$$I(\lambda_1)/I(\lambda_2) = [A(\lambda_1)/A(\lambda_2)] \times [\lambda_2/\lambda_1].$$

Table 4 compares observed values with those predicted by a number of theories. Among the former are observed ratios taken from the line intensities reported by Selvelli et al. (2007) for data from the STIS and UVES instruments but for which no error bars are given. These can be compared with the RLIR values with rather large error bars, and those from the Isaac Newton telescope (INT) reported by Liu & Danziger (1993). The latter are mean values of intensity ratios from about 12 objects with all values of equal weight. Probable error estimates are provided. The theories are presented by method: variational Breit–Pauli (TFF and FF), analytic Breit–Pauli (AHK), and distorted wave (BK) including the spin-orbit effect.

Table 4
A Comparison of Observed and Predicted Intensity Ratios for Pairs of Bowen Lines Originating from the Same Upper Level

Line Ratios	Observation				Theory			
	STIS	UVES	RLIR	INT	TFF	FF	AHK	BK
2810.5/3122.5	0.177				0.101	0.095	0.119	0.106
3406.7/3416.2		0.81			0.762	0.773	1.08	0.851
3416.2/3122.5		0.15			0.145	0.139	0.115	0.090
3431.6/3122.5		0.169			0.188	0.193	0.164	0.119
2819.5/3445.0	0.0348				0.0396	0.0368	0.048	0.0326
2837.1/3445.0	0.38				0.402	0.382	0.439	0.435
3133.7/3445.0	3.18	3.12	3.02 ± 0.57	3.33 ± 0.16	3.342	3.208	3.67	4.06
3429.6/3445.0	0.15	0.14		0.185 ± 0.035	0.154	0.154	0.191	0.181
3048.0/3024.3	3.17				3.13	3.15	3.07	3.05
3060.2/3036.3	2.00				1.91	1.89	1.78	1.71
3313.3/3341.7	0.75	0.74	0.723 ± 0.172	0.693 ± 0.036	0.736	0.738	0.682	0.661
3300.3/3341.7	0.29	0.28	0.314 ± 0.075	0.253 ± 0.046	0.268	0.265	0.242	0.230
3300.3/3313.3	0.38	0.38		0.365	0.364	0.362	0.353	0.348
3792.4/3755.8		0.29	0.267 ± 0.030	0.268 ± 0.040	0.299	0.298	0.306	0.312
3775.1/3758.3			0.717 ± 0.201	0.573 ± 0.085	0.704	0.706	0.714	0.714

Notes. Lines are designated by vacuum wavelengths (Å). Sources are as follows: STIS and UVES (Selvelli et al. 2007), RLIR (Djeniže et al. 2003), INT (Liu & Danziger 1993), TFF (Tachiev & Froese Fischer 2001), FF (Froese Fischer 1994), AHK (Aggarawal et al. 1997), BK (Bhatia & Kastner 1993).

We have independently measured the *HST*/STIS lines that were listed in Table 4 of Selvelli et al. (2007). The original RR Tel observations were made under *HST* program 8098 (PI: Francis Keenan). The fully calibrated "x1d" files were retrieved in 2008 June from the *HST* archives. In general, we find very good agreement with the Selvelli et al. emission line intensities. There is one important exception where we measure 4.82×10^{-13} erg cm^{-2} s^{-1} while their entry is 2.37×10^{-13} erg cm^{-2} s^{-1} for the $\lambda_{air} = 3023.45$ Å line. This was measured with the E230M echelle grating from data set O5EH01090. Two orders (2 and 3) cover this line. We use only order 3 while Selvelli et al. used an automated procedure that averaged the two orders in the wavelength regions with order overlap (P. Selvelli 2008, private communication). The line in order 2 is poor. For this line, we use our own value; otherwise we use Selvelli et al. entries in their Table 4 for compiling the intensities in our Table 4 in the STIS and UVES columns. Following Selvelli et al., we also make no extinction corrections under the assumption that it is negligible for RR Tel.

In Table 4, the first column labels the line intensity ratio using vacuum wavelengths to promote ease in identification with theoretical values. We have ordered the various line ratios by grouping them according to the upper level in decreasing order. The highest level for which well observed lines arise is the $2p3d\ ^3P^o_1$ level that is 329583.89 cm^{-1} above the ground state. Sets are separated by a blank line as we continue down the energy-level ladder.

We have tried to apply objective criteria when deciding what line ratios to enter in Table 4. We consider only those ratios where both lines have reasonably high signal-to-noise ratios. For instance, the $\lambda_{vac} = 3025.421$ Å line is excluded because the intensity measurement is not sufficiently accurate to use as a test of *A*-values. Even with the STIS echelle, it is still not well separated at the base from the brighter blue-side line at $\lambda_{vac} = 3024.306$ Å. Some of the line ratios in Table 4 are not independent (they can be formed from other entries) but are presented to facilitate intercomparisons. There are a total of 21 Bowen lines used in the table, ranging in wavelength from 2810.5 to 3792.4 Å.

Some differences between the STIS and UVES sets of observed data are noted but these could be accommodated by relatively small error bars. The error bars for RLIR ratios are often 2–4 times as large as those for INT.

Very clearly the most discrepant intensity ratio by far in Table 4 is for the comparison in the first row, the 2810.5/3122.5 ratio. The ratio 0.177 determined from the STIS spectra is a factor of 1.75 higher than our recommended theoretical prediction of 0.101 (TFF column). Otherwise, there is generally good agreement. A possible cause is that the O III 2810.486 Å line is blended. There is a definite asymmetry to the line shape on the red side. This feature was measured with the E230M echelle grating from data set O5EH01090. We fit the line with a Gaussian profile that yielded a line center wavelength of 2809.903 Å and a FWHM of 39 km s^{-1} (0.37 Å). Applying the radial velocity of RR Tel of -61.8 km s^{-1} (http://simbad.u-strasbg.fr/simbad/sim-fid), we find a line center wavelength of 2810.482 Å vacuum rest wavelength in excellent agreement with O III 2810.486.

We examined Peter Van Hoof's line list (http://www.pa.uky.edu/~peter/newpage/) for likely identifications of a putative blend. A reasonable candidate is the [Fe III] line at 2810.71 Å (vacuum). This transition $3d^54s\ ^5P_3 - 3d^6\ ^1G_4$ arises on level 40, 66464.64 cm^{-1} above ground. We are unaware of transition probabilities for this or any other line that originates on this upper level. Hence, further discussion of this possible contaminating feature is beyond the scope of this paper. Nevertheless, the possibility of a significant contribution to the STIS measured flux by an unidentified line(s) is a reason to not judge the theoretical predicted 2810.5/3122.5 intensity ratio as imprecise.

Table 4 shows that the Breit–Pauli values have changed somewhat: the near-perfect agreement between STIS and FF values for the 2837/3445 ratio has not been preserved. The present value for the 3134/3445 ratio is larger than the earlier

Table 5
Breit–Pauli and MCDHF M1 Transition Rates (in s^{-1})

Transition Rate	Breit–Pauli	MCDHF	
		I	II
$10^3 A(4960)$	6.946	6.525	6.526
$10^2 A(5008)$	2.025	1.950	1.968

value but is in excellent agreement with the INT value. The largest difference in data from observed INT sources is found for 3775/3758 where all theories are in near-perfect agreement with the RLIR value.

7. E2 AND M1 RELATIVE INTENSITIES

[O III] lines for $2p^2\ ^3P_J - {}^1D_2$, $J = 0, 1, 2$ transitions with vacuum wavelengths 4932.603, 4960.295, 5008.240 Å, respectively, have been found in spectra of the Orion Nebula (Baldwin et al. 2000; Esteban et al. 2004) and relative intensities measured. A spectrum of comparable quality has also been measured for the Galactic H II region NGC 3576 (García-Rojas et al. 2004).

For the $I(5008)/I(4960)$ intensity ratio, the Breit–Pauli data (Tachiev & Froese Fischer 2001) predicted a ratio of 2.919 in close agreement with other theory (Galavís et al. 1997). Most of the intensities of these lines arise from M1 components of the emission for which it has been shown (Drake 1971) that there are relativistic corrections to the transition operator that, in some circumstances, may be important. Storey & Zeippen (2000) computed these corrections to the Galavís et al. (1997) data and obtained a ratio in better agreement with observation. As a check on the Breit–Pauli calculations, separate multiconfiguration Dirac–Hartree–Fock (MCDHF) calculations were performed using the GRASP2K code Jönsson et al. (2007). The expansions were similar to the MCHF expansions described in Section 2 except that the 1*s* shell was always filled. MCDHF calculations grow more rapidly than nonrelativistic expansions and the code does not allow as much variation in the orbitals as the set increases, resulting in a slower convergence. Two methods of optimization were used—simultaneous optimization where the same orbital set is used for all four levels, and independent optimization. These methods will be referred to as MCDHF I and II, respectively. The results from the former were quite stable as the expansion size was increased whereas the latter had a slow, but regular convergence pattern that, when extrapolated, agreed well with the former. Comparing the M1 transition rates from the Breit–Pauli and two MCDHF methods, Table 5 shows small but significant differences between the uncorrected Breit–Pauli and the MCDHF results.

Table 6 compares relative line intensities from observation with similar ratios from theory. Only observational values for [O III] 4932.603 Å that deblend this line from [Fe III] 4931.91 Å and that rely on spectra of high quality have been used. The observed values for the $I(4933)/I(4960)$ ratios in Table 6 are in reasonable agreement with the average value derived by Mathis & Liu (1999) using several low-resolution observations that suffer uncertainty from the blending with the [Fe III] line: $I(4933)/I(4960) = (4.15 \pm 0.11) \times 10^{-4}$ for eight planetary nebulae. Among the theoretical values, the first two are uncorrected Breit–Pauli values. The MCDHF II values are somewhat larger than MCDHF I. E2 transition probabilities are much more difficult to determine accurately than the M1 transition probabilities and account for most of the variation

Table 6
Line Intensities from Various Sources

$I(5008)/I(4960)$	$I(4933)/I(4960)$	Ref.
Observation		
2.966	3.82e-04	Baldwin et al. (2000)
3.00		Rubin et al. (2003)
2.994	4.06e-04	Esteban et al. (2004)
2.909	4.20e-04	García-Rojas et al. (2004)
Theory		
2.89	2.50e-04	Galavís et al. (1997)
2.919	3.341e-04	Tachiev & Froese Fischer (2001)
2.984		Storey & Zeippen (2000)
2.964	3.533e-04	MCDHF I
2.993	4.082e-04	MCDHF II
2.992	3.556e-04	BP* I
3.016	3.558e-04	BP* II

in the two sets of values. There are no relativistic corrections to the E2 transition operator in the length form for Breit–Pauli calculations that include many-body effects more accurately. In Table 6, we include intensity ratios BP* I and II that merely replaced the M1 transition probabilities by the MCDHF I and II values, respectively. There is excellent agreement with observations for both BP* values for the intensity ratio of the two bright lines. The $I(5008)/I(4960)$ ratio is determined primarily by M1 transition rates, whereas the agreement of the ratio involving the weak line at 4933 Å that decays only through an E2 transition, though improved over earlier theory, is less certain.

From a theoretical point of view, the accuracy of computed transition probabilites for emission lines from $2p^2\ ^1D_2$ is similar to those for lines from $2p^2\ ^1S_0$. The lifetime of the latter level is $\tau = 1/[A(E2; {}^3P_2) + A(M1; {}^3P_1) + A(E2; {}^1D_2)]$ where the transitions to ^3P are LS forbidden while the transition to $^1D_2$ is LS allowed. Generally, theoretical LS-allowed transition probabilities are more accurate than LS forbidden, and M1 transition probabilities more accurate than E2. The contribution to the lifetime from the E2 LS-forbidden transition is negligible. In Table 2, the lifetime of the $^1S_0$ level is compared with laboratory measurements. There are large uncertainties in experimental values, but the difference between the value quoted by Träbert et al. (2000) and theory is 1%. If we assume similar errors for the lines from $^1D_2$, and that lines are either both overestimated or under-estimated (which is reasonable since both are $^1D - {}^3P$ transitions) and a 10% error for the weak line that decays only through an E2 LS-forbidden transition, we obtain the estimate of 2.99 ± 0.03 for $I(5008)/I(4960)$ and $(3.56 \pm 0.36) \times 10^{-4}$ for $I(4933)/I(4960)$. Comparison with the mean and standard error of the observed values in Table 6, 2.97 ± 0.02 and $(4.0 \pm 0.1) \times 10^{-4}$, suggests the uncertainties for the latter may be larger.

8. CONCLUSION

An in-depth analysis of the most recent Breit–Pauli transition data for O III (Tachiev & Froese Fischer 2001) has been reported. The accuracy of the energy levels has improved significantly compared with earlier results (Froese Fischer 1994) and the agreement in the length and velocity forms of the line strength is now a few percent for many transitions. Comparisons with experiment and other theory confirm the reliability of the data that agree with STIS or UVES data generally within 5%–7%. There is excellent agreement with the present value for the 3313/3342 ratio and the RLIR ratio specially recommended

by Djeniže et al. (2003) as their measurement with the highest accuracy for lines within cascades in the Bowen fluorescence mechanism.

We are grateful to Xiao-wei Liu for providing some past history regarding the observations and theory pertaining to the $\lambda_{air} = 4931$ Å line. We thank NASA Ames summer students Julia Fang and Patrick Maher for their help measuring the *HST*/STIS spectral lines. Partial support for this publication was provided by NASA through Program number HST-AR-10973.01-A (PI RR) from the Space Telescope Science Institute, which is operated by the Association of Universities for Research in Astronomy, under NASA contract NAS5-26555. M.R. acknowledges support from Mexican CONACYT project 50359-F.

REFERENCES

Aggarawal, K. M., Hibbert, A., & Keenan, F. P. 1997, ApJS, 108, 393 (AHK)
Baldwin, J., Verner, E. M., Verner, D. A., Ferland, G. J., Martin, P. G., Korista, K. T., & Rubin, R. H. 2000, ApJS, 129, 229
Baudinet-Robinet, Y., Dumont, P. D., & Garnir, H. P. 1991, Phys. Rev. A, 43, 4022
Bhatia, A. K., & Kastner, S. O. 1993, At. Data Nucl. Data Tables, 54, 133
Djeniže, S., Bukvič, S., Srećković, A., & Kalezić, S. 2003, A&A, 406, 759
Drake, G. W. F. 1971, Phys. Rev. A, 3, 908
Esteban, C., Peimbert, M., García-Rojas, J., Ruiz, M. T., Peimbert, A., & Rodríguez, M. 2004, MNRAS, 355, 229
Fleming, J., & Brage, T. 1997, J. Phys. B, 30, 1385
Fleming, J., Hibbert, A., & Stafford, R. P. 1994, Phys. Scr., 49, 316
Froese Fischer, C. 1981, Phys. Scr., 23, 38
Froese Fischer, C. 1994, Phys. Scr., 49, 51 (FF)
Froese Fischer, C. 2009, Phys. Scr., T134, 014019
Froese Fischer, C., Brage, T., & Jönsson, P. 1997, Computational Atomic Structure (Bristol: IOP)
Froese Fischer, C., & Tachiev, G. 2002, The MCHF/MCDHF Collection (Nashville, TN: Vanderbilt Univ.), http://atoms.vuse.vanderbilt.edu
Froese Fischer, C., & Tachiev, G. 2004, At. Data Nucl. Data Tables, 87, 1
Froese Fischer, C., Tachiev, G., Gediminas, G., & Godefroid, M. R. 2007, Comput. Phys. Commun., 176, 597
Galavís, M. E., Mendoza, C., & Zeippen, C. J. 1998, A&AS, 123, 159
García-Rojas, J., Esteban, C., Peimbert, M., Rodríguez, M., Ruiz, M.-T., & Peimbert, A. 2004, ApJS, 153, 501
Johnson, C., & Smith, P. 1984, ApJ, 281, 477
Jönsson, P., He, X., Froese Fischer, C., & Grant, I. P. 2007, Comput. Phys. Commun., 176, 597
Kastner, S. O., & Bhatia, A. K. 1990, ApJ, 362, 745
Kastner, S. O., & Bhatia, A. K. 1996, MNRAS, 279, 1137 (KB)
Liu, X.-W., & Danziger, J. 1993, MNRAS, 261, 465
Luo, D., Pradhan, A. K., Saraph, H. E., Storey, P. J., & Yu, Y. 1989, J. Phys. B, 22, 389
Mathis, J. S., & Liu, X.-W. 1999, ApJ, 521, 212
Nahar, S. 1998, Phys. Rev. A, 58, 3766
Pinnington, E. H., Donnelly, K. E., & Irwin, D. J. G. 1978, Can. J. Phys., 56, 508
Pinnington, E. H., Irwin, D. J. G., Livingston, A. E., & Kernahan, J. A. 1974, Can. J. Phys., 52, 1961
Ralchenko, Yu., et al. 2008, NIST Atomic Spectra Database (version 3.1.5; Gaithersburg, MD: NIST), http://physics.nist.gov/asd3
Rubin, R. H., Martin, P. G., Dufour, R. J., Ferland, G. J., Blagrave, K. P. M., Liu, X.-W., Nguyen, J. F., & Baldwin, J. A. 2003, MNRAS, 340, 362
Selvelli, P., Danziger, J., & Bonifacio, P. 2007, A&A, 464, 71
Smith, S. J., Čadež, I., Chutjian, A., & Nimura, M. 2004, ApJ, 402, 1075
Storey, P. J., & Zeippen, C. J. 2000, MNRAS, 312, 813
Tachiev, G., & Froese Fischer, C. 2001, Can. J. Phys., 79, 955 (TFF)
Träbert, E., Calamai, A. G., Gillaspy, J. D., Gwinner, G., Tordoir, X., & Wolf, A. 2000, Phys. Rev. A, 62, 022507
Wiese, W. L., Fuhr, J., & Deters, T. M. 1996, J. Chem. Phys. Ref. Data, Monograph 7